http://dx.doi.org/10.5012/bkcs.2012.33.2.670

Effect of Overlayer Thickness of Hole Transport Material on Photovoltaic Performance in Solid-Sate Dye-Sensitized Solar Cell

Hui-Seon Kim,[†] Chang-Ryul Lee,[†] In-Hyuk Jang,[†] Weekyung Kang,[‡] and Nam-Gyu Park[†,*]

[†]*School of Chemical Engineering and Department of Energy Science, Sungkyunkwan University, Suwon 440-746, Korea*
[*]*E-mail: npark@skku.edu*
[‡]*Department of Chemistry, Soongsil University, Seoul 156-743, Korea*
Received January 26, 2012, Accepted January 31, 2012

The photovoltaic performance of solid-state dye-sensitized solar cells employing hole transport material (HTM), 2,2',7,7'-tetrakis-(*N*,*N*-di-*p*-methoxyphenyl-amine)-9,9'-spirobifluorene (spiro-MeOTAD), has been investigated in terms of HTM overlayer thickness. Two important parameters, soak time and spin-coating rate, are varied to control the HTM thickness. Decrease in the period of loading the spiro-MeOTAD solution on TiO_2 layer (soak time) leads to decrease in the HTM overlayer thickness, whereas decrease in spin-coating rate increases the HTM overlayer thickness. Photocurrent density and fill factor increase with decreasing the overlayer thickness, whereas open-circuit voltage remains almost unchanged. The improved photocurrent density is mainly ascribed to the enhanced charge transport rate, associated with the improved charge collection efficiency. Among the studied HTM overlayer thicknesses, *ca.* 230 nm-thick HTM overlayer demonstrates best efficiency of 4.5% at AM 1.5G one sun light intensity.

Key Words : Solid-state dye-sensitized solar cell, Hole transport, Spiro-MeOTAD, Overlayer thickness, Electron transport

Introduction

Dye-sensitized Solar Cells (DSSCs) have attracted lots of interests due to high solar-to-electricity conversion efficiency, low cost and facile fabrication process. The first DSSC developed by O'Regan and Grätzel in 1991 was based on the liquid electrolyte employing iodide/triiodide redox couple.[1] Since then, many alternatives such as organic redox electrolytes (TEMPO[2] or sulfur contained one[3-5]) and metal (cobalt, iron, or copper) based complexes[6-9] have been developed to overcome the disadvantage of iodide/triiodide redox couple, such as corrosiveness, and to maximize the open-circuit voltage determined by potential difference between the conduction band of metal oxide and the redox potential of electrolyte. However, DSSC employing liquid electrolyte itself shows drawbacks related to the stability problem. It was reported that the relatively volatile electrolyte shows poor stability in severe environmental condition,[10] which encourages solid-state DSSCs to be developed. Solid-state DSSC has almost same structure with DSSC employing liquid electrolyte except that the electrolyte is replaced by a hole transport material (HTM). In 1998 organic hole transport material of 2,2',7,7'-tetrakis-(*N*,*N*-di-*p*-methoxyphenyl-amine)-9,9'-spirobifluorene (spiro-MeOTAD) was introduced by Bach *et al.*[11] and it is still considered as one of the best candidates for HTM.

While preparing solid-state DSSC using a spin-coating technology, infiltration of spiro-MeOTAD into the mesoporous TiO_2 film has been issued since filling fraction is known to be important parameter in determining the photovoltaic characteristics. Snaith *et al.* reported that once HTM solution was penetrated into mesoporous film by capillary action, it diffused into the deeper mesoporous film by concentration gradient given by the evaporation of the solvent at the surface during the spin-coating process.[12] It was also pointed out that the pore filling would be terminated when solvent was completely evaporated and HTM became immobile. The filling fraction is therefore expected to be strongly dependent on the HTM solution concentration, the TiO_2 film thickness and/or porosity and the spin-coating rate. Under the condition of the spiro-MeOTAD concentration (180 mg in 1 mL chlorobenzene), the soak time of 1 min and the spin-coating rate of 2000 rpm, *ca.* 60-65% filling fraction could be achieved with 2.8 μm-thick TiO_2 film.[13] During the pore filling process, the entire HTM thickness is expected to be influenced as well. When considering the mean free path of the spiro-MeOTAD being determined to be less than 4 μm,[14] the HTM overlayer at a given TiO_2 film thickness must be considered as a crucial factor. However, little investigation has been made on the dependence of photovoltaic property on the HTM overlayer thickness. Here we report on the effect of the HTM overlayer thickness on photovoltaic performance. HTM soak time and spin-coating rate are varied to control the HTM overlayer thickness. Change of photovoltaic performance with HTM overlayer thickness is investigated with transient photocurrent spectroscopy.

Experimental

6 mM *cis*-disothiocyanato-(2,2'-bipyridyl-4,4'-dicarboxylic acid)-(2,2'-bipyridyl-4,4'-dinonyl) ruthenium(II) (coded Z907, Everlight) was prepared in 1-methoxy-2-propanol, to

which 6 mM 4-guanidinobutyric acid (GBA, 98%, Aldrich), was added. Anatase TiO_2 nanoparticles were synthesized by acetic acid catalyzed hydrolysis of titanium isopropoxide (97%, Aldrich), followed by autoclaving at 230 °C for 12 h.[15] Aqueous solvent in the autoclaved TiO_2 colloid solution was replaced by ethanol for preparation of non-aqueous TiO_2 paste. Ethyl cellulose (Aldrich), lauric acid (Fluka), and terpineol (Aldrich) were added into the ethanol solution of the TiO_2 particles, and then ethanol was removed from the solution using a rotary evaporator to obtain viscous pastes. For homogeneous mixing, the paste was further treated with a three-roll mill. The nominal composition of TiO_2/terpineol/ethylcellulose/lauric acid was 1/6/0.3/0.1. Fluorine-doped tin oxide (FTO) glasses (Pilkington, TEC-8, 8 Ω/sq) were cleaned in an ultrasonic bath containing ethanol for 15 min. To make a compact TiO_2 blocking layer, 0.15 M titanium diisopropoxide bis(acetylacetonate) (75 wt %, Aldrich) in 1-butanol (Aldrich) solution was spin-coated on the cleaned FTO glass and heated at 125 °C for 5 min, which was repeated twice. The nanocrystalline TiO_2 paste was deposited on the compact TiO_2 blocking layer using a screen-printing method, followed by annealing at 550 °C for 1 h to obtain mesoporous TiO_2 film. The sintered TiO_2 films were immersed in 0.02 M aqueous $TiCl_4$ (Aldrich) solution at 80 °C for 15 min, which was heated at 500 °C for 15 min. Prepared films were immersed in the Z907 dye solution at room temperature for 10 min. The composition of hole transport material (HTM) was 0.17 M 2,2',7,7'-tetrakis-(*N*,*N*-di-*p*-methoxyphenyl-amine)-9,9'-spirobifluorene (spiro-MeOTAD, Merck), 0.0328 M bis(trifluoromethane)sulfonimide lithium salt (LiTFSI, 99.95%, Aldrich) and 0.19 M 4-*tert*-butylpyridine (TBP, 96%, Aldrich) in the mixed solvent of chlorobenzene (99.8%, Aldrich) and acetonitrile (99.8%, Aldrich) (chlorobenzene:acetonitrile = 1:0.05 v/v). The HTM solution was loaded on the Z907 sensitized TiO_2 film, which was followed by spin-coating at rate ranging from 1500 to 2500 rpm. For the positive electrode, a 160 nm-thick Ag (99.99%, Kurt J. Lesker) was deposited on the top of the HTM overlayer in a thermal evaporator system where *ca.* 10^{-6} torr vacuum condition was maintained. The active area was measured by a digital camera (DCMe 500) and analyzed by an image analysis program (Leopard 2009). The TiO_2 film thickness was measured by alpha-step IQ surface profile (KLA Tencor). The HTM overlayer thicknesses were measured by a field-emission scanning electron microscope under accelerating voltage of 15 kV (FE-SEM, JEOL, JSM-7600F).

Photocurrent and voltage were measured by a solar simulator (Oriel Sol 3A class AAA) equipped with 450 W xenon lamp (Newport 6279NS) and a Keithley 2400 source meter. The NREL-calibrated Si solar cell with KG-2 filter was used to adjust light intensity into one sun illumination (100 mW/cm^2). The time constants for charge transport and recombination were measured by using a photocurrent and photovoltage transient setup. The cells were probed with a weak laser pulse at 532 nm superimposed on a relatively large, back ground (bias) illumination at 680 nm. The details on the transient setup and data collection were described elsewhere.[15]

Results and Discussion

Figure 1 shows cross sectional SEM images of the mesoporous TiO_2 films infiltrated with HTM. The HTM overlayer forms at the top of the mesoporous film as shown in Figures 1(a)-(f), where it is clearly seen that the overlayer thickness increases as the soak time increases from 15 s to 150 s at the give spin-coating rate of 2500 rpm. The mesopores at the vicinity of FTO layer are filled with HTM, which indicates that the spiro-MeOTAD molecules are well

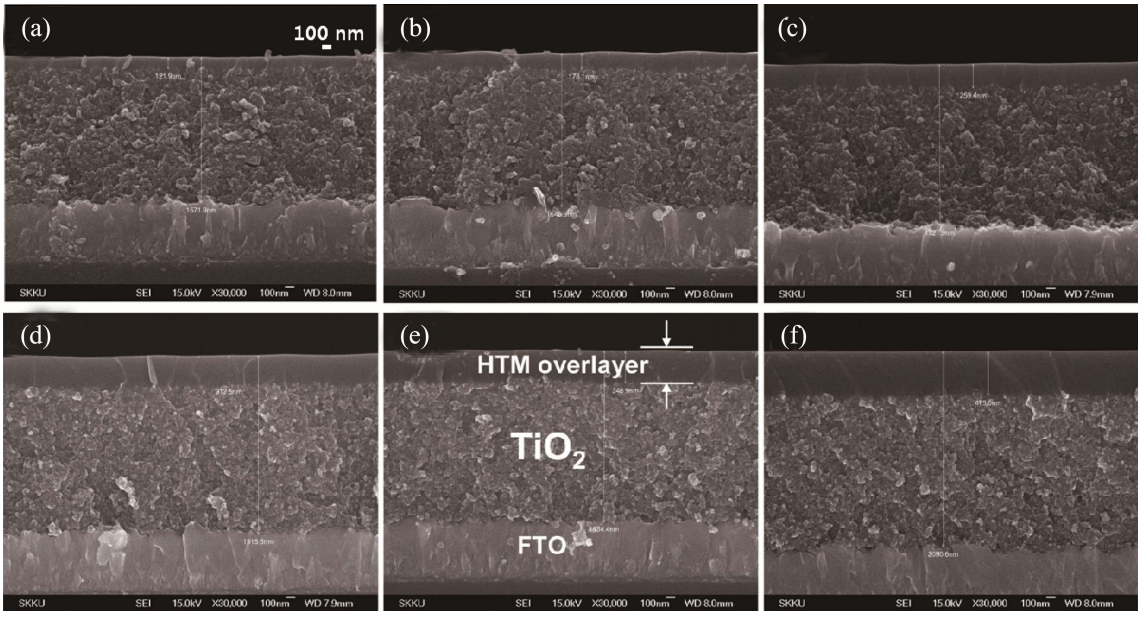

Figure 1. Cross sectional SEM images of the 1.8 μm-thick mesoporous TiO_2 films infiltrated with spiro-MeOTAD HTM soaked for (a) 15 s, (b) 30 s, (c) 60 s, (d) 90 s, (e) 120 s, and (f) 150 s at the spin-coating rate of 2500 rpm.

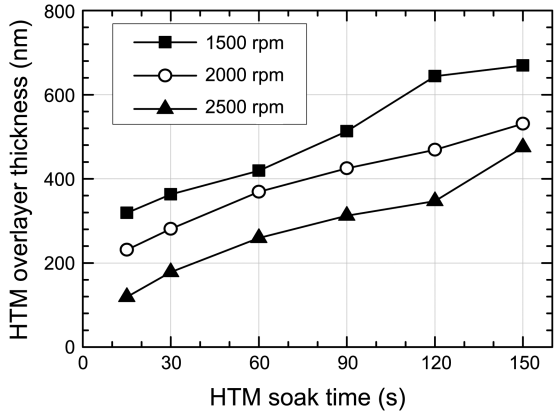

Figure 2. Dependence of the HTM overlayer thickness on soak time and spin-coating rate.

infiltrated into the entire 1.8 μm-thick TiO_2 film. This result agrees well with the fact that mesoporous TiO_2 film < 2 μm enables its pore to be efficiently filled with HTM.[16] It is found that the thickness can be controlled between 100 and 700 nm depending on spin-coating condition such as soak time and spin-coating rate.

Figure 2 and Table 1 show the effect of soak time on the HTM overlayer thickness at different spin-coating rate. At the given spin-coating rate, the thickness increases lineally with increasing the soak time. At the given soak time, the faster the spin-coating rate is, the thinner the overlayer becomes. For example, the HTM thickness decreases from 319 nm to 231 nm and to 119 nm as the spin-coating rate increases from 1500 rpm to 2000 rpm and to 2500 rpm, respectively, for the soak time of 15 s. It was reported that the spin-coating rate was found to have also influence on filling fraction, where filling faction was improved with decreasing spin-coating rate and such an improvement of filling fraction led to thick overlayer.[13] Since the HTM overlayer thickness is likely to correlate with the pore filling fraction, it is necessary to investigate and compare the photovoltaic performance for the different coating condition.

Measured I-V curves and photovoltaic parameters are presented in Figure 3 and Table 2, respectively. It is found that photocurrent density (J_{SC}) decreases gradually as the soak time increases from 15 s to 150 s, whereas open-circuit voltage (V_{OC}) seems to be independent on the soak time. Fill factor (FF) is also deteriorated with increasing the soak time. When comparing the spin-coating rate, the degree of change in J_{SC} is more pronounced for 1500 rpm than that for 2000 rpm. For the given spin-coating rate of 1500 rpm, J_{SC} shows 9.4 mA/cm^2 for 15 s soak time, which is unremittingly declined to 6.1 mA/cm^2 as the soak time increases up to 150 s. Whereas, in case of 2000 rpm, J_{SC} of 11.2 mA/cm^2 observed for 15 s soak time is slightly decreased to about 10.2 mA/cm^2 as the soak time increases up to 90 s. For the longer soak time of 150 s, J_{SC} is gradually declined to 9.3 mA/cm^2. In case of 2500 rpm, J_{SC} decreases similarly with increasing the soak time (data not shown here), however, it is much lower than that of 1500 or 2000 rpm at the given soak time or for the similar overlayer thickness. Maximum J_{SC} of 8.9 mA/cm^2 is obtained at 2500 rpm for 30 s soak time. It is obvious that the HTM overlayer thickness has the significant influence on photocurrent density and thin overlayer is beneficial to high J_{SC}. Moreover, it is notable that for the similar HTM

Table 1. The HTM overlayer thickness depending on soak time and spin-coating rate

	HTM overlayer thickness (nm)		
Soak time (s)	1500 rpm	2000 rpm	2500 rpm
15	319	231	119
30	363	281	178
60	419	369	259
90	513	425	312
120	644	469	347
150	669	531	475

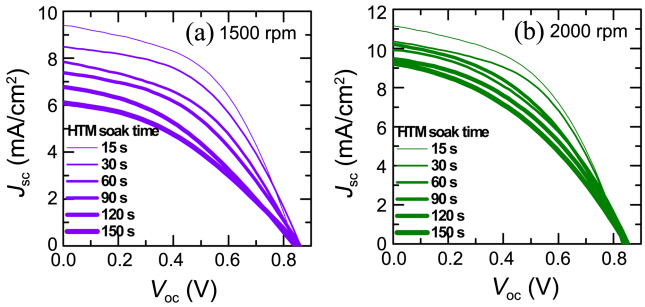

Figure 3. Dependence of photocurrent density (J_{SC})-open-circuit voltage (V_{OC}) curves on soak time at (a) 1500 rpm and (b) 2000 rpm.

Table 2. Photocurrent density (J_{SC}), open-circuit voltage (V_{OC}), fill factor (FF), and conversion efficiency (η) of solid-state DSSC depending on soak time at 1500 and 2000 rpm

1500 rpm					2000 rpm				
Soak time (s)	J_{SC} (mA/cm^2)	V_{OC} (V)	FF	η (%)	Soak time (s)	J_{SC} (mA/cm^2)	V_{OC} (V)	FF	η (%)
15	9.4	0.841	0.49	3.9	15	11.2	0.830	0.48	4.5
30	8.5	0.861	0.48	3.5	30	10.4	0.834	0.49	4.2
60	7.8	0.851	0.44	3.0	60	9.9	0.857	0.42	3.6
90	7.4	0.860	0.42	2.7	90	10.2	0.841	0.43	3.7
120	6.8	0.841	0.38	2.2	120	9.4	0.846	0.41	3.3
150	6.1	0.857	0.38	2.0	150	9.3	0.847	0.39	3.0

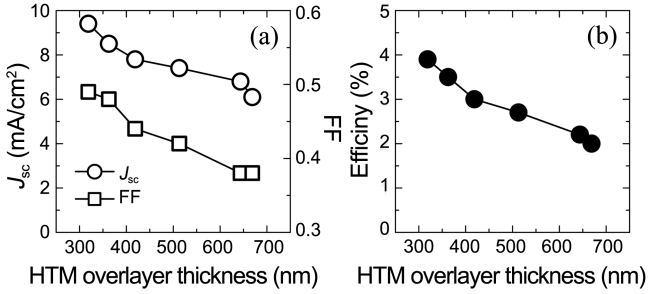

Figure 4. (a) Photocurrent density (*J*sc), fill factor (FF), and (b) conversion efficiency as a function of HTM overlayer thickness for the case of 1500 rpm.

thickness such as 363 nm (30 s at 1500 rpm) and 369 nm (60 s at 2000 rpm) the J_{SC} is not similar (8.5 mA/cm^2 for 30 s at 1500 rpm and 9.9 mA/cm^2 for 60 s at 2000 rpm), which suggests that soak time plays more important role in determining photovoltaic performance than spin-coating rate, which may be associated with filling faction.

In Figure 4 photovoltaic parameters obtained from 1500 rpm are plotted as a function of the HTM overlayer thickness. J_{SC} and FF increase by 54% and 29%, respectively, as the overlayer thickness decreases by about 52%, which leads to increase in conversion efficiency by 95% from 2.0% to 3.9%. In the case of 2000 rpm, similar tendency is observed but, as mentioned previously, the decreasing rate in J_{SC} is not so prominent as 1500 rpm case. It was found that increase in HTM overlayer thickness led to large series resistance and thereby low FF.[17] Therefore, the lowered FF with increasing the soak time is likely to be related to the increased series resistance. For the change in J_{SC}, it is noted that J_{SC} is significantly affected by the change in the HTM overlayer thickness in spite of no change in TiO_2 thickness and dye loading. To verify the increase in J_{SC} with decreasing overlayer thickness, charge transport property is investigated using transient photocurrent spectroscopy.

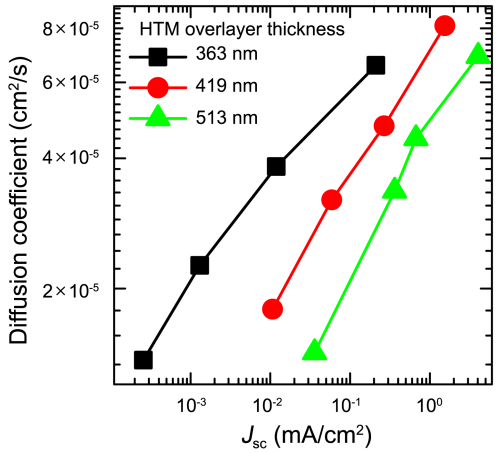

Figure 5. Effect of the HTM overlayer thickness on electron diffusion coefficient (D) obtained from the equation, $D = d^2/(2.35 \cdot \tau_c)$, where time constant for electron transport (τ_c) and film thickness (d = 1.8 μm) were measured by transient photocurrent spectroscopy and alpha-step IQ surface profiler.

Figure 5 shows electron diffusion coefficient as a function of light intensity, represented by J_{SC}. Decrease in the overlayer thickness from 513 to 363 nm improves electron diffusion coefficient (D) that is calculated from $D = d^2/(2.35 \cdot \tau_c)$, where τ_c and d represent time constant for electron transport and TiO_2 film thickness (d = 1.8 μm), respectively. Whereas, time constant for charge recombination (τ_r) shows negligible difference (figure is not shown), which is consistent with no change in voltage with overlayer thickness. Consequently diffusion length (L), $L = (D \cdot \tau_r)^{1/2}$, and charge collection efficiency (η_{cc}), $\eta_{cc} = 1 - (\tau_c/\tau_r)$, are dominated by τ_c. Thus, decrease in τ_c (increase in D) by decreasing overlayer thickness is responsible for the increased J_{SC}, associated with the improved charge collection efficiency. It was found that the hole mobility of spiro-MeOTAD was independent of the sample thickness over the range of thicknesses from 0.135 mm up to 4 mm.[14] The current in non-crystalline medium is generally known to be proportional to the product of the number density of the charge carrier and the drift speed of charge carrier, where the drift speed of charge carrier is proportional to the product of mobility and electric field in the medium. Considering that the electric field is the voltage difference per unit distance in the medium, the J_{SC} is related to the thickness of HTM layer because applied voltage is not much varied at the studied HTM overlayer thickness ranging from *ca.* 0.2 mm to *ca.* 0.7 mm as shown in Table 2. Thus, it can be postulated that J_{SC} will decrease with increasing the overlayer thickness since the drift speed of holes decreases with increasing the HTM layer thickness. The decreased hole drift speed with increasing the HTM overlayer thickness retards probably the electron transport rate in the TiO_2 matrix.

Conclusion

In solid-state DSSC employing the HTM spiro-MeOTAD, the HTM overlayer thickness was found to have a significant effect on photocurrent density and fill factor but little effect on photovoltage. Photocurrent density and fill factor were deteriorated as the HTM thickness increased. The HTM overlayer thickness was controlled either by soak time or spin-coating rate. Increases in the soak time led to increase in the HTM overlayer thickness. On the other hand, increase in the spin-coating rate resulted in decrease in the HTM overlayer thickness. Overlayer thicknesses produced by short soak time and slow spin-coating rate was as similar as those obtained by relatively longer soak time and faster spin-coating rate, however, photovoltaic performance was different. Although the HTM overlayer thickness was almost the same, higher photocurrent density was obtained from deposition of HTM layer by longer soak time and faster spin-coating rate, which might be related to pore filling fraction depending on HTM coating condition. It is concluded from this study that enough soak time and fast spin-coating rate are simultaneously important in relation with high pore filling fraction and adequate HTM overlayer thickness.

Acknowledgments. This work was supported by the National Research Foundation of Korea (NRF) grant funded by the Ministry of Education, Science and Technology (MEST) of Korea under contract No. 2011-0016441 and the Korea Institute of Energy Technology Evaluation and planning (KETEP) grant funded by the Ministry of Knowledge Economy under contract No. 20103020010010. H.-S.K. is grateful to global PhD fellowship grant from NRF under contract No. 2011-0008467.

References

1. O'Regan, B.; Grätzel, M. *Nature* **1991**, *353*, 737.
2. Zhang, Z.; Chen, P.; Murakami, T. N.; Zakeeruddin, S. M.; Grätzel, M. *Adv. Funct. Mater.* **2008**, *18*, 341.
3. Wang, M.; Chamberland, N.; Breau, L.; Moser, J.-E.; Humphry-Baker, R.; Marsan, B.; Zakeeruddin, S. M.; Grätzel, M. *Nat. Chem.* **2010**, *2*, 385.
4. Li, D.; Li, H.; Luo, Y.; Li, K.; Meng, Q.; Armand, M.; Chen, L. *Adv. Funct. Mater.* **2010**, *20*, 3358.
5. Tian, H.; Jiang, X.; Yu, Z.; Kloo, L.; Hagfeldt, A.; Sun, L. *Angew. Chem. Int. Ed.* **2010**, *49*, 7328.
6. Nusbaumer, H.; Moser, J.-E.; Zakeeruddin, S. M.; Nazeeruddin, Md. K.; Grätzel, M. *J. Phys. Chem. B* **2001**, *105*, 10461.
7. Hattori, S.; Wada, Y.; Yanagida, S.; Fukuzumi, S. *J. Am. Chem. Soc.* **2005**, *127*, 9648.
8. Daeneke, T.; Kwon, T.-H.; Holmes, A. B.; Duffy, N. W.; Bach, U.; Spiccia, L. *Nat. Chem.* **2011**, *3*, 213.
9. Kim, H.-S.; Ko, S.-B.; Jang, I.-H.; Park, N.-G. *Chem. Comm.* **2011**, *47*, 12637.
10. Sommeling, P. M.; Spath, M.; Smit, H. J. P.; Bakker, N. J.; Kroon, J. M. *J. Photochem. Photobio. A* **2004**, *164*, 137.
11. Bach, U.; Lupo, D.; Comte, P.; Moser, J.-E.; Weissortel, F.; Salbeck, J.; Spreitzer, H.; Grätzel, M. *Nature* **1998**, *395*, 583.
12. Snaith, H. J.; Humphry-Baker, R.; Chen, P.; Cesar, I.; Zakeeruddin, S. M.; Grätzel, M. *Nanotech.* **2008**, *19*, 424003.
13. Ding, I.-K.; Tetreault, N.; Brillet, J.; Hardin, B. E.; Smith, E. H.; Rosenthal, S. J.; Sauvage, F.; Grätzel, M.; McGehee, M. D. *Adv. Funct. Mater.* **2009**, *19*, 2431.
14. Poplavskyy, D.; Nelson, J. *J. Appl. Phys.* **2003**, *93*, 341.
15. Kim, M.-J.; Lee, C.-R.; Jeong, W.-S.; Im, J.-H.; Ryu, T. I.; Park, N.-G. *J. Phys.Chem. C* **2010**, *114*, 19849.
16. Kroeze, J. E.; Hirata, N.; Schmidt-Mende, L.; Orizu, C.; Ogier, S. D.; Carr, K.; Grätzel, M.; Durrant, J. R. *Adv. Funct. Mater.* **2006**, *16*, 1832.
17. Fabregat-Santiago, F.; Bisquert, J.; Palomares, E.; Otero, L.; Kuang, D.; Zakeeruddin, S. M.; Grätzel, M. *J. Phys. Chem. C* **2007**, *111*, 6550.